Using SWAT to simulate streamflow in Huifa River basin with ground and Fengyun precipitation data

Honglei Zhu, Ying Li, Zhaoli Liu, Xiaoliang Shi, Bolin Fu and Zefeng Xing

ABSTRACT

High-resolution satellite precipitation products, which can provide a reasonable depiction of the spatial extent of rainfall, have been increasingly used to model hydrological processes. In this study, we introduced important satellite rainfall data – Fengyun (FY) precipitation product, and evaluated the data through streamflow simulation using the Soil and Water Assessment Tool model in Huifa River basin, China. Three precipitation inputs were conducted to investigate the simulation performance of the FY precipitation product: (1) available rain gauges within the watershed; (2) pixel values of FY-2 precipitation products nearest to the geographic centers of the subbasins; and (3) mean values of FY-2 precipitation pixels within the subbasins. The results showed that good model performance (defined as: NSE > 0.75; Nash–Sutcliffe efficiency: NSE) was achieved for all precipitation inputs both in the calibration and validation period. Best streamflow simulation was obtained when the model was calibrated with the third precipitation input, with NSE 0.86 and 0.84, R^2 0.86 and 0.86 in the calibration and validation period. This study reveals that the FY precipitation product is a significant data source in modeling hydrological processes. Moreover, it is reasonable to use the mean values of the satellite precipitation pixels within the subbasins.

Key words | Fengyun (FY) precipitation product, precipitation input, rainfall, remote sensing, streamflow, SWAT

Honglei Zhu
Ying Li (corresponding author)
Zhaoli Liu
Bolin Fu
Zefeng Xing
Northeast Institute of Geography and Agricultural Ecology,
Chinese Academy of Sciences,
Shengbei Road 4888,
Changchun 130102,
China
E-mail: *liying@neigae.ac.cn*

Honglei Zhu
Bolin Fu
Zefeng Xing
University of Chinese Academy of Sciences,
Beijing 100049,
China

Xiaoliang Shi
College of Geomatics,
Xi'an University of Science and Technology,
Xi'an 710054,
China

INTRODUCTION

Precipitation is often identified as the most important variable in modeling watershed streamflow. Most commonly used watershed models (such as SWAT, AGNPS and TOPMODEL) are designed to readily incorporate data from rain gauges. The model performance is strongly influenced by the density of the rain gauge network (Sun *et al.* 2002; Anctil *et al.* 2006; Xu *et al.* 2013). As a traditional data source of precipitation, rain gauge networks are usually not able to fully represent the spatial pattern of rainfall (Strauch *et al.* 2012). Remote-sensing technologies potentially provide a reasonable depiction of the spatial extent of precipitation at the watershed scale (Tobin & Bennett 2013). Hydrologists are attracted by the growing availability of high-resolution satellite precipitation products, particularly in developing countries and remote locations where weather radars are absent and conventional rain gauges are sparse (Bitew *et al.* 2012).

Three satellite rainfall products are most widely used to drive simulations, which include tropical rainfall measuring mission (TRMM) multi-satellite precipitation analysis (TMPA) method near-real-time (3B42RT) product, TMPA method post-real-time research version (3B42) and climate prediction center morphing method. Studies have been conducted by hydrologists in different places using these satellite rainfall products (Yu *et al.* 2011; Wagner *et al.* 2012; Tobin & Bennett 2013, 2014). A consensus was obtained that satellite rainfall products were a considerable precipitation data source for streamflow simulation. Bitew *et al.* (2012) summarized the studies that have evaluated satellite rainfall products through streamflow simulation and

doi: 10.2166/hydro.2015.104

indicated that: satellite rainfall products have potential use for hydrological applications; model performance depends on satellite product type, watershed size and hydroclimatic region; and model performance increases when the model is calibrated with satellite rainfall input rather than with rain gauge input.

As the first generation of geostationary orbit meteorological satellite, FY-2 meteorological satellites and the polar orbit meteorological satellites constitute the Chinese meteorological satellite application system. FY-2 meteorological satellites launched from 1997 to 2012 include two test satellites (FY-2A satellite, satellite FY-2B) and four business satellites (FY-2C satellite, FY-2D satellite, FY-2E satellite, satellite FY-2F), which are used to: (1) obtain the day, day and night, visible-light cloud infrared cloud water distribution; (2) broadcast weather map; and (3) collect meteorological, hydrological and marine monitoring data from a meteorological data collection platform. FY-2 meteorological satellites are an important tool in global information collecting, severe weather and environmental monitoring, meteorological service and earth system science research (Shu *et al.* 2011; Rasmussen *et al.* 2014; Yang *et al.* 2014; Liu *et al.* 2015). FY-2 satellites have launched many atmosphere products, including FY precipitation products. However, there is almost no relevant literature of the precipitation data used in hydrological simulation.

For this paper, the Soil and Water Assessment Tool (SWAT) model was selected, which is a distributed parameter continuous time model developed by the United States Department of Agriculture, Agricultural Research Service (Arnold *et al.* 1996, 1998). The SWAT model uses the data of a precipitation gauge nearest to the centroid of each subcatchment as an input for that subcatchment. Each grid cell of remote-sensing precipitation data is input into the model as a virtual precipitation site (Price *et al.* 2014). For TRMM data, for example, the grid size is $0.25 \times 0.25\,^{\circ}$, and one subbasin may contain one or a few grid cells. Compared with TRMM data, the grid size of FY precipitation data is $0.1 \times 0.1\,^{\circ}$, which means one subbasin may contain more grid cells. It is not reasonable for high spatial resolution remote-sensing precipitation data (e.g., FY precipitation data) that only grid cells closest to the geographic centers of the subbasins are used.

Therefore, this study, taking the Huifa River basin as a case study, simulates the streamflow using ground and FY precipitation data with SWAT. The study aims to: (1) evaluate the streamflow simulation accuracy of FY precipitation data, and (2) discuss how to make full use of high precision remote-sensing precipitation data in SWAT.

STUDY AREA

Huifa River is the second largest tributary of Songhua River and the main water source to Songhua Lake water. The Huifa River basin with an area of 12,385 km^2 is located in the northeast of China (Figure 1). The watershed has complex topography with elevations ranging from 172 to 1,391 m. The distribution of rainfall in Huifa River basin is uneven in a year. The rainfall is concentrated in summer and autumn, and precipitation in July and August accounts for 44.7% of the annual rainfall. Runoff behavior is characterized by three important regimes: the high-flow period that occurs in spring due to snow and ice melt; the high flow that occurs in summer as a result of high rainfall; and the low-flow period that occurs during the winter.

DATA AND METHODS

FY-2 precipitation data processing

FY-2 precipitation data are derived from FY-2C, FY-2D and FY-2E satellite images, assisted by the ground observation data with an estimation method. The method is developed by Yu *et al.* (http://www.nsmc.cma.gov.cn/NSMC/Contents/100250.html), and has two steps: (1) establish the relationship between cloud top temperature and precipitation; (2) calibrate the estimated satellite precipitation data with the ground observation data. FY-2 precipitation data include four time resolution products: 1-hour, 3-hours, 6-hours and 24-hours precipitation product. In this study, FY-2C/D 24-hours precipitation data from 2006 to 2010 were used. The spatial range of the data is 0–50 °N, 55–155 °E.

Figure 2 shows the FY-2 C/D precipitation data processing flow. The original FY-2 C/D precipitation data do not

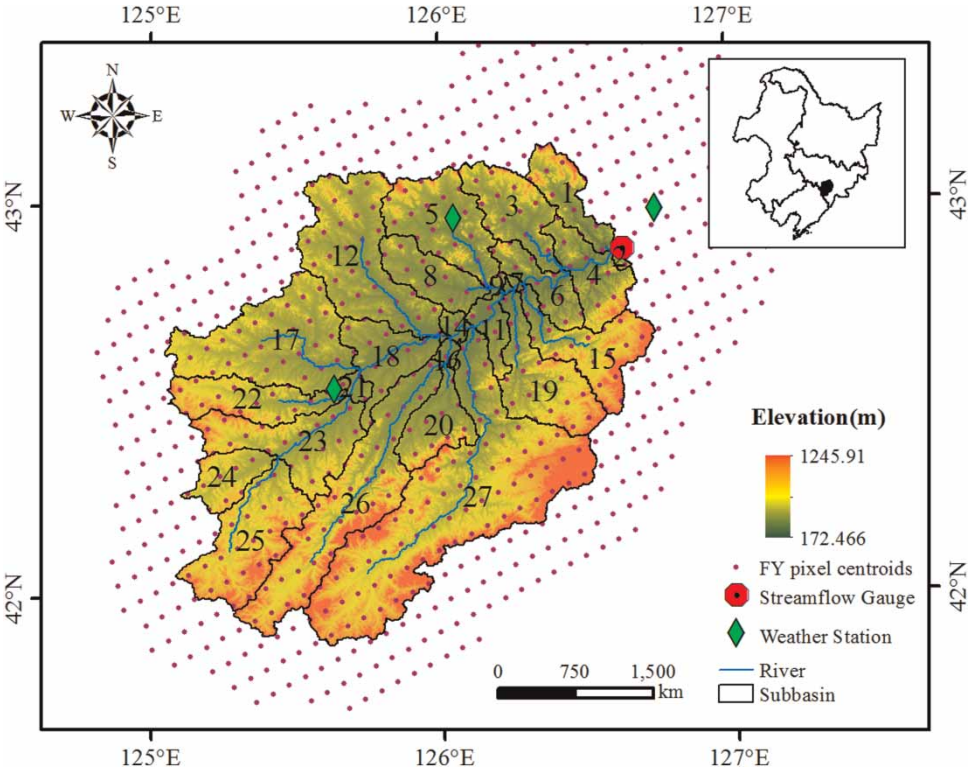

Figure 1 | The location of Huifa watershed.

have coordinate information. A geometric correction needs to be done with a geographic lookup table (GLT) file. The GLT file contains map locations for every pixel of the image it is associated with. It consists of two bands: sample numbers and line numbers of the georeferenced image. Pixel values indicate the sample or line number of the pixel in the original input image that belongs at the given map location in the output image.

Two GLT files of FY-2 C/D were generated with a geographic information (latitude and longitude in decimal degrees) file supported by FENGYUN Satellite Data Center (http://satellite.cma.gov.cn/PortalSite/StaticContent/DocumentDownload.aspx?TypeID=3) using the Build GLT tool in ENVI 4.8. A batch program was edited with ENVI/IDL, and the 1,826 images were georeferenced with the GLT files.

Then, we obtained the daily precipitation of the virtual rain gauges with Zonal Statistics As Table tool using ArcGIS 10.0 and Python. Zonal Statistics As Table tool summarizes the values of a raster within the zones of another data set and reports the results to a dbf file. A zone can be a cell of FY precipitation data or a subbasin. Finally, the dbf files were converted to the txt format of SWAT input precipitation.

SWAT model description

SWAT has been successfully applied all over the world for solving various processes including streamflow, climate change, erosion and sedimentation, agricultural non-point source pollution, water resources and land management (Jayakrishnan *et al.* 2005; Schaffner *et al.* 2009; Shen *et al.* 2009; Easton *et al.* 2010; Niraula *et al.* 2013; Zhang *et al.* 2013). SWAT is a conceptual, process-based, long-term continuous watershed scale simulation model. Input information for SWAT is grouped or organized into the following categories: climate; hydrologic response units (HRUs); ponds/wetlands; groundwater; and the main channel, or reach, draining the subbasin. The model subdivides a watershed into subbasins connected by a stream network and further into HRUs. The HRUs possessing unique land use/cover, soil and slope attributes are non-spatially

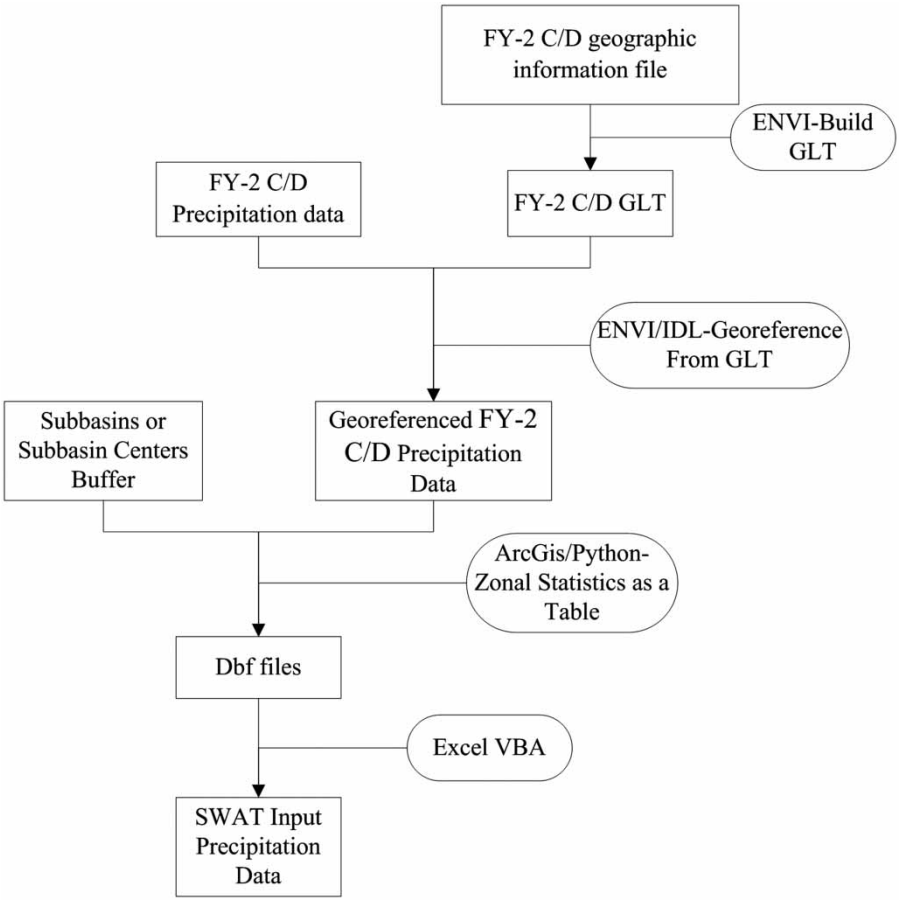

Figure 2 | FY-2 C/D precipitation data processing flow.

distributed assuming there is no interaction and dependency (Neitsch *et al.* 2005). Runoff is predicted separately for each HRU and routed to obtain the total runoff for the watershed. The hydrologic cycle is based on the water balance equation

$$\mathrm{SW}_t = \mathrm{SW}_0 + \sum_{i=1}^{t} (R_i - Q_i - \mathrm{ET}_i - \mathrm{Pe}_i - \mathrm{QR}_i) \quad (1)$$

where SW_t is the final soil water content (mm H_2O), SW_0 is the initial soil water content on day i (mm H_2O), t is the time (days), R_i is the amount of precipitation on day i (mm H_2O), ET_i is the amount of evapotranspiration on day i (mm H_2O), Pe_i is the amount of water entering the vadose zone from the soil profile on day i (mm H_2O), QR_i is the amount of return flow on day i (mm H_2O).

SWAT input data

Precipitation input data

In this study, three different precipitation inputs were applied to simulate the streamflow of Huifa River basin.

- Case 1: precipitation data of three rain gauges (Huadian, Meihekou and Panshi).
- Case 2: pixel values of FY-2 precipitation products nearest to the geographic centers of the subbasins.
- Case 3: a virtual rain gauge is created in each subbasin. Mean values of FY-2 precipitation pixels within the subbasins are regarded as the virtual rain gauges' precipitation.

Model inputs

SWAT version 2012 with an ArcGIS 10.0 user interface was used in this paper. SWAT model requires inputs on topography, land use/land cover, soils, weather and management and some additional factors. The Shuttle Radar Topography Mission DEM of 90 m resolution was used for subbasin definition. Two per cent of the watershed area was used as the threshold for the delineation of subbasins. A total of 27 subbasins were delineated in the study area. Land use/land cover data for the year 2005 were derived from Landsat5 TM images (2005) by visual interpretation in ArcGIS 10.0. Land uses in this watershed are 43% forest, 32% corn, 15% rice and 10% other uses including urban areas, pasture and water. Soils data were obtained from China Soil Scientific Database (http://www.soil.csdb.cn/page/index.vpage). The major soil in the watershed is dark-brown earth (34%), followed by albic soil (28%) and meadow soil (12%). Three categories of slope were defined to be used in the HRU definition, that is, (1) 0–3.12, (2) 3.12–17.49 and (3) 17.49–9,999. The slope classification was derived from an unsupervised classification method in ENVI 4.8.

Finally, after overlaying the land use, soil and slope maps, a threshold value of 5% for land use, soil and slope was used in the HRU definition. A threshold value of 5–10% is generally used in HRU definition to avoid small HRUs, reduce total number of HRUs, and improve computational efficiency of the model (Tobin & Bennett 2009; Masih *et al.* 2011). A total of 682 HRUs were delineated in the study area.

Meteorological input, except rainfall (i.e., temperature, wind, humidity and sunshine hours), was obtained from the China Meteorological Data Sharing Service System (http://cdc.cma.gov.cn/home.do). Monthly observed streamflow data were obtained from Wudaogou hydrologic station.

Model calibration

The formulated SWAT models for three cases scenarios were independently calibrated using SWAT-CUP (calibration and uncertainty programs). SWAT-CUP is a public domain program linking the sequential uncertainty fitting, version 2 (SUFI-2) procedure to SWAT. SUFI-2 is recognized as a robust tool for generating combined calibration and uncertainty analysis of the SWAT model (Schuol *et al.* 2008; Akhavan *et al.* 2010; Azimi *et al.* 2013; Sloboda & Swayne 2013; Setegn *et al.* 2014).

In SWAT, there are 26 parameters sensitive to water flow. The 26 parameters were adjusted in each sensitivity test using the Latin Hypecube, One-Factor-At-a-Time method (Van Griensven *et al.* 2006). Parameter sensitivity changed with the different precipitation inputs. A sensitivity analysis (300 simulations) was conducted for each precipitation data set. Table 1 lists the most sensitive model parameters identified by this procedure used to develop, calibrate and validate the model.

Coefficient of determination (R^2), the Nash–Sutcliffe efficiency (NSE) (Nash & Sutcliffe 1970) and bias (%bias) were selected to evaluate the goodness of fit between the observations and the final best simulation. R^2, NSE and bias are calculated using the following equations:

$$\%\text{Bias} = \frac{Q_{\text{sim}} - Q_{\text{obs}}}{Q_{\text{obs}}} 100\% \tag{2}$$

$$\text{NSE} = 1 - \frac{\sum (Q_{\text{obs}} - Q_{\text{sim}})^2}{\sum (Q_{\text{obs}} - \overline{Q_{\text{sim}}})^2} \tag{3}$$

$$R^2 = \frac{\left(\sum (Q_{\text{obs}} - \overline{Q_{\text{obs}}})(Q_{\text{sim}} - \overline{Q_{\text{sim}}})\right)^2}{\sum (Q_{\text{obs}} - \overline{Q_{\text{obs}}})^2 \sum (Q_{\text{sim}} - \overline{Q_{\text{sim}}})^2} \tag{4}$$

where Q_{obs} is the observed discharges, $\overline{Q_{\text{obs}}}$ is the mean of observed discharges, Q_{sim} is the simulated discharges, $\overline{Q_{\text{sim}}}$ is the mean of simulated discharges.

RESULTS AND DISCUSSION

Accuracy assessment of FY-2 precipitation data

Pixels in the FY-2 precipitation data where the three rain gauges were located were extracted to evaluate the

Table 1 | SWAT calibration parameters

Variable	Description	Sensitivity rank		
		Case 1	Case 2	Case 3
CN2	SCS runoff curve number f	1	1	1
ALPHA_BF	Baseflow alpha factor (days)	2	8	8
ESCO	Soil evaporation compensation factor	3	9	6
CH_K2	Effective hydraulic conductivity in main channel alluvium	4	10	9
EPCO	Plant uptake compensation factor	5	13	13
CH_N2	Manning's 'n' value for the main channel	6	7	5
CANMX	Plant uptake compensation factor	7	2	2
GW_DELAY	Groundwater delay (days)	8	6	7
SOL_Z	Depth from soil surface to bottom of layer	9	3	3
GWQMN	Threshold depth of water in the shallow aquifer required for return flow to occur (mm)	10	5	11
GW_REVAP	Groundwater 'revap' coefficient	11	11	10
SOL_K	Saturated hydraulic conductivity	12	12	4
SOL_AWC	Available water capacity of the soil layer	13	4	12

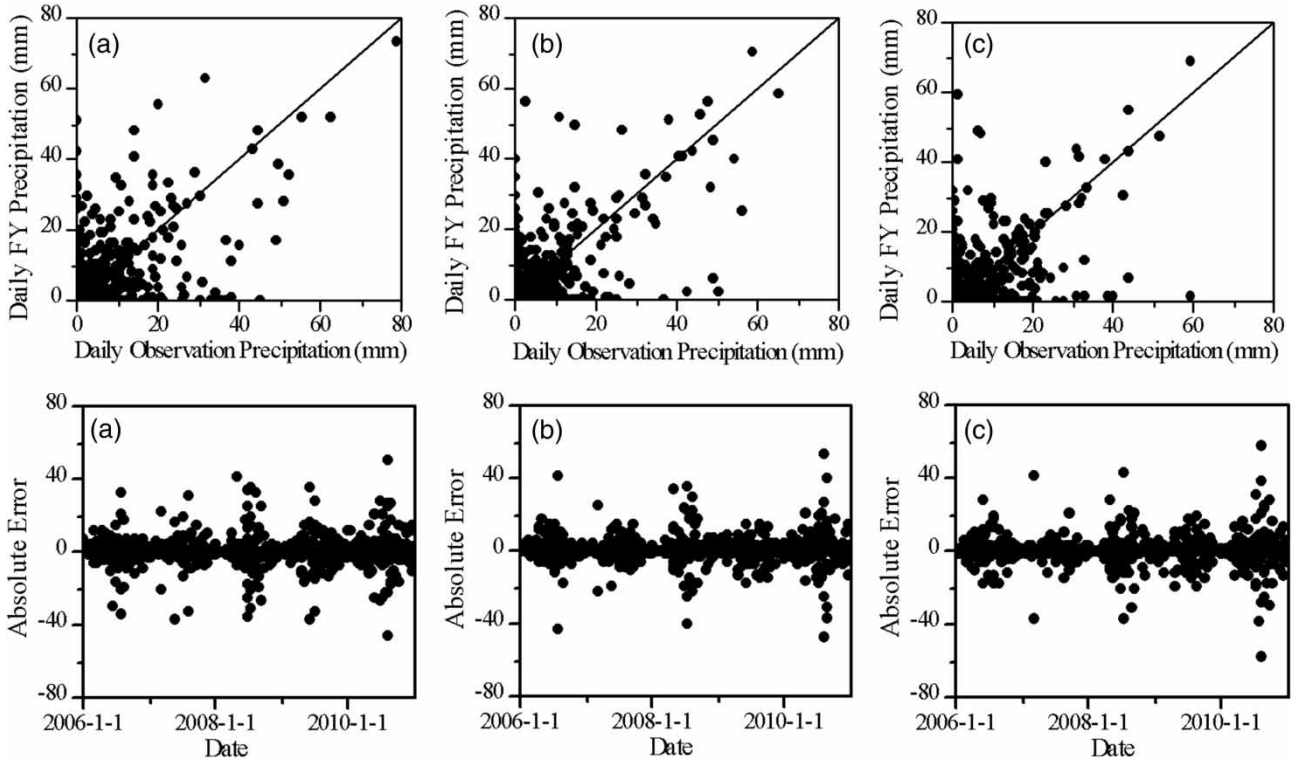

Figure 3 | Comparison of daily observed precipitation and FY-2 precipitation data: (a) Huadian, (b) Meihekou, and (c) Panshi.

precipitation estimate accuracy. The evaluation was conducted daily and monthly from the year 2006 to 2010. Figure 3 shows the comparison of daily observed precipitation and FY-2 precipitation data. A correlation

coefficient (r) was used to describe the estimate accuracy of FY-2 precipitation data. It is defined as follows:

$$r = \frac{\left(\sum (P_{obs} - \overline{P_{obs}})(P_{FY} - \overline{P_{FY}})\right)^2}{\sum (P_{obs} - \overline{P_{obs}})^2 \sum (P_{FY} - \overline{P_{FY}})^2} \quad (5)$$

where P_{obs} is the observed precipitation, $\overline{P_{obs}}$ is the mean of observed precipitation, P_{FY} is the FY estimated precipitation, $\overline{P_{FY}}$ is the mean of FY estimated precipitation.

FY-2 precipitation data showed a normal performance on estimating daily rainfall, with correlations of 0.56, 0.70 and 0.69, respectively. Further analysis of the absolute errors among the three rain gauges indicated that absolute errors ranged from −60 to 60 mm and almost became larger in summer, which may be related to seasonal precipitation over the watershed.

Comparison of monthly observed precipitation and FY-2 precipitation data was also applied (Figure 4). FY-2 precipitation data showed a promising estimate on monthly precipitation, with correlations of 0.97, 0.98 and 0.99.

Comparison of precipitation input

The mean annual precipitation for the three precipitation inputs was calculated (Figure 5(a)–5(c)). Case 1 precipitation, ranging from 713 to 787 millimeters per annum (mm/a), was divided into three parts in space due to only using three rain gauges (Figure 5(a)). Higher mean annual precipitation was observed in Case 2 (Figure 5(b)) and Case 3 (Figure 5(c)) with a range from 778 to 1,000 mm/a, which indicated an overestimate in the FY precipitation products. Moreover, the pattern of rainfall for Case 2 and Case 3 presented as being variable in space. Precipitation in the lower part of the basin was larger than the upper part.

Figure 5(d)–5(f) shows the differences in the mean annual precipitation among the three cases. There was a significant difference (from 44 to 279 mm) between Case 1 and Case 2, also between Case 1 and Case 3 (from 49 to 279 mm). Similar rainfall in space was observed in Figure 5(f), with a difference ranging from −31 to 31 mm. A further analysis of precipitation within the subbasins was conducted. Figure 6 shows the daily standard deviation of FY precipitation within subcatchments 14 and 27, which covered an area of 57 and 2,419 km^2, respectively. The daily standard deviation for subbasins 14 and 27 was in the range of 0–9 and 0–18. It indicated that the difference in precipitation became larger with increasing area. Moreover, it suggested that the precipitation input using pixels nearest to the centroid of subcatchments may not result in reliability of streamflow simulation.

Comparison of streamflow simulation

The SWAT model was run at a monthly scale. The calibration period was done for the years 2006–2008 with the first year as the warm up period and the validation using the 2009–2010 period.

Statistical analysis and comparison of simulation error for each data set are displayed in Table 2. According to the performance classification of Moriasi *et al.* (2007), very good model performance (defined as: NSE > 0.75) was achieved for all precipitation inputs both in the calibration and validation period. The simulation based on Case 1

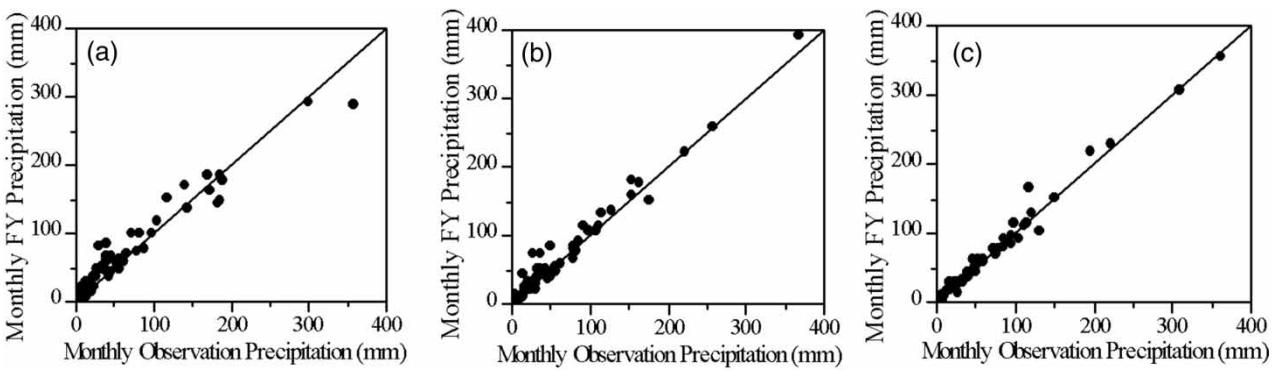

Figure 4 | Comparison of monthly observed precipitation and FY-2 precipitation data: (a) Huadian, (b) Meihekou, and (c) Panshi.

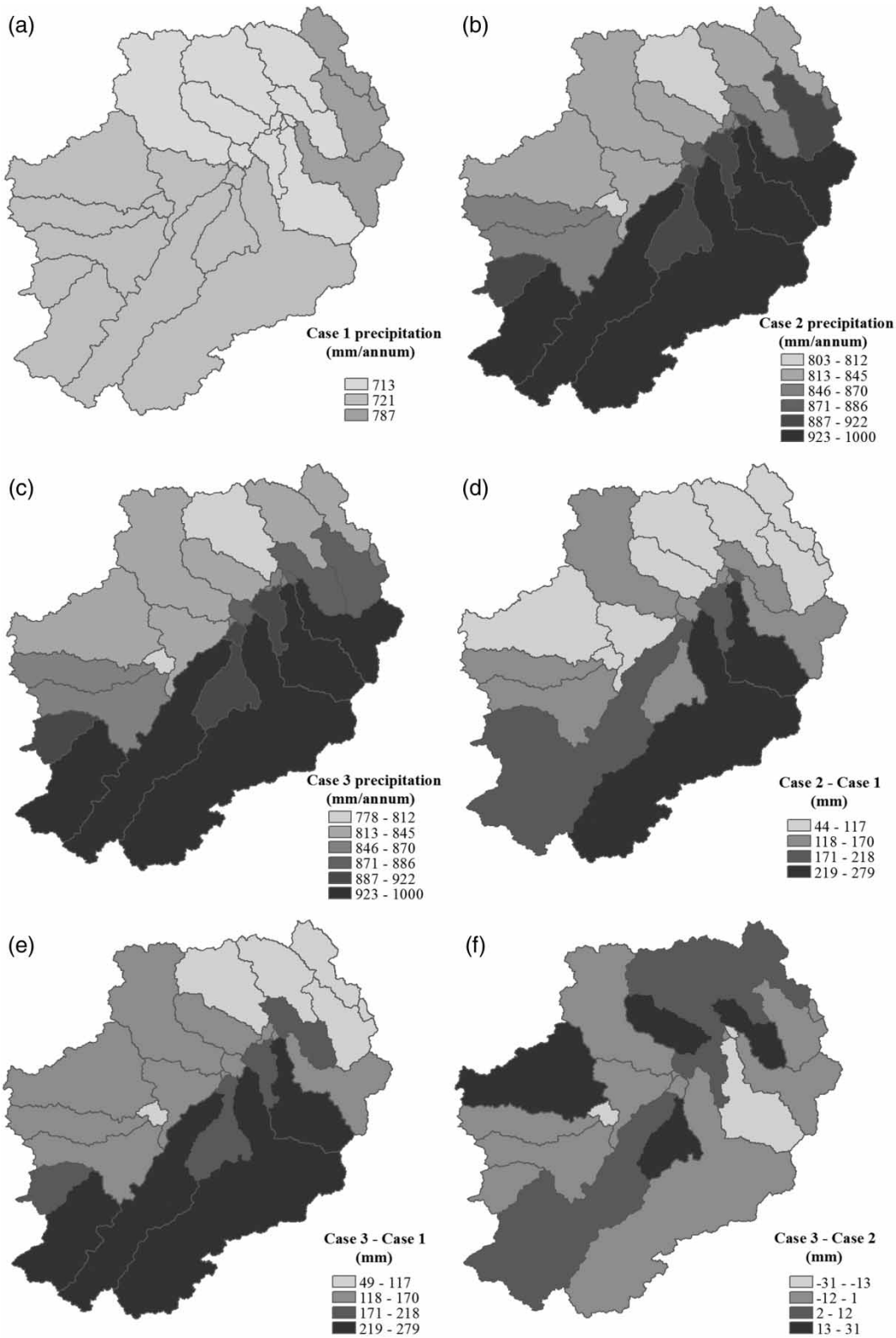

Figure 5 | Mean annual precipitation for Case 1 (a), Case 2 (b), and Case 3 (c), differences among Case 1 (d), Case 2 (e), and Case 3 (f).

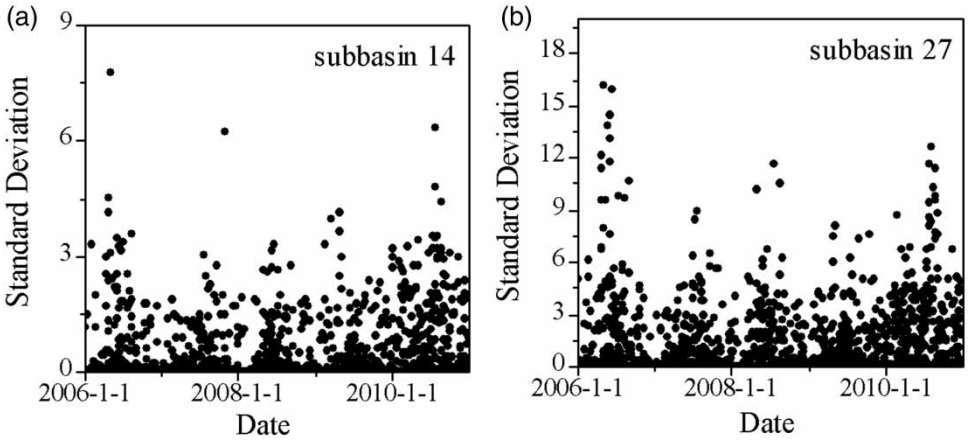

Figure 6 | The daily standard deviation of FY precipitation within subbasins 14 and 27.

Table 2 | Error comparison of the hydrological modeling

		Mean value			
	Period	$\overline{Q_{obs}}$	$\overline{Q_{sim}}$	R^2	Nash index
Case 1	Calibration	51.34	50.42	0.83	0.83
	Validation	124.14	100.92	0.87	0.8
Case 2	Calibration	51.34	52.24	0.84	0.84
	Validation	124.14	139.38	0.84	0.83
Case 3	Calibration	51.34	49.93	0.86	0.86
	Validation	124.14	128.37	0.86	0.84

precipitation input (rain gauges) was satisfying, with Nash index 0.83 and 0.8, R^2 0.83 and 0.87 in the calibration and validation period. However, a large bias was observed in the validation period (bias = 18.7). The R^2 and NSE values for Case 2 precipitation input (pixel values of FY-2 precipitation products nearest to the geographic centers of the subbasins) were stable in calibration ($R^2 = 0.84$ and NSE = 0.84) and validation ($R^2 = 0.84$ and NSE = 0.83) phases, but the bias was a little greater (12.3%) in the validation phase. The hydrological model driven by Case 3 precipitation data (mean values of FY-2 precipitation pixels within the subbasins) performed better than Case 1 and Case 2 precipitation data, with Nash index 0.86 and 0.84, R^2 0.86 and 0.86 in the calibration and validation periods. A little bias was observed in the simulation using Case 3 precipitation input (−2.7% for calibration and 3.4% for validation). Model hydrographs for each precipitation input are shown in Figure 7.

CONCLUSION

In this study, we compared the accuracy of SWAT streamflow simulations using FY high-resolution satellite rainfall product and rain gauge data in Huifa River basin. Performance was compared under three precipitation inputs: (1) rain gauges; (2) pixel values of FY-2 precipitation products nearest to the geographic centers of the subbasins; and (3) mean values of FY-2 precipitation pixels within the subbasins. The results indicated that SWAT performed watershed simulations reasonably well with all precipitation inputs ($R^2 > 0.8$ and NSE ≥ 0.8). Significant improvements were obtained when the model was calibrated with FY precipitation product rather than with rain gauge data. Moreover, the simulation generated from Case 3 precipitation input performed better than from Case 2 precipitation input. The streamflow simulation is more reasonable using mean values of satellite precipitation pixels within subbasins. The results suggested that FY precipitation product was a practical data source for hydrological modeling at a monthly time scale in watersheds with limited rain gauges.

As a result of lacking daily observed streamflow data, the model was conducted at monthly scale. From the foregoing analysis, it revealed that correlations were lower between FY precipitation values and rain gauge values at the daily time scale (0.56, 0.70 and 0.69). It is unknown how streamflow simulation driven by FY precipitation product performed at the daily time scale. Moreover, estimate

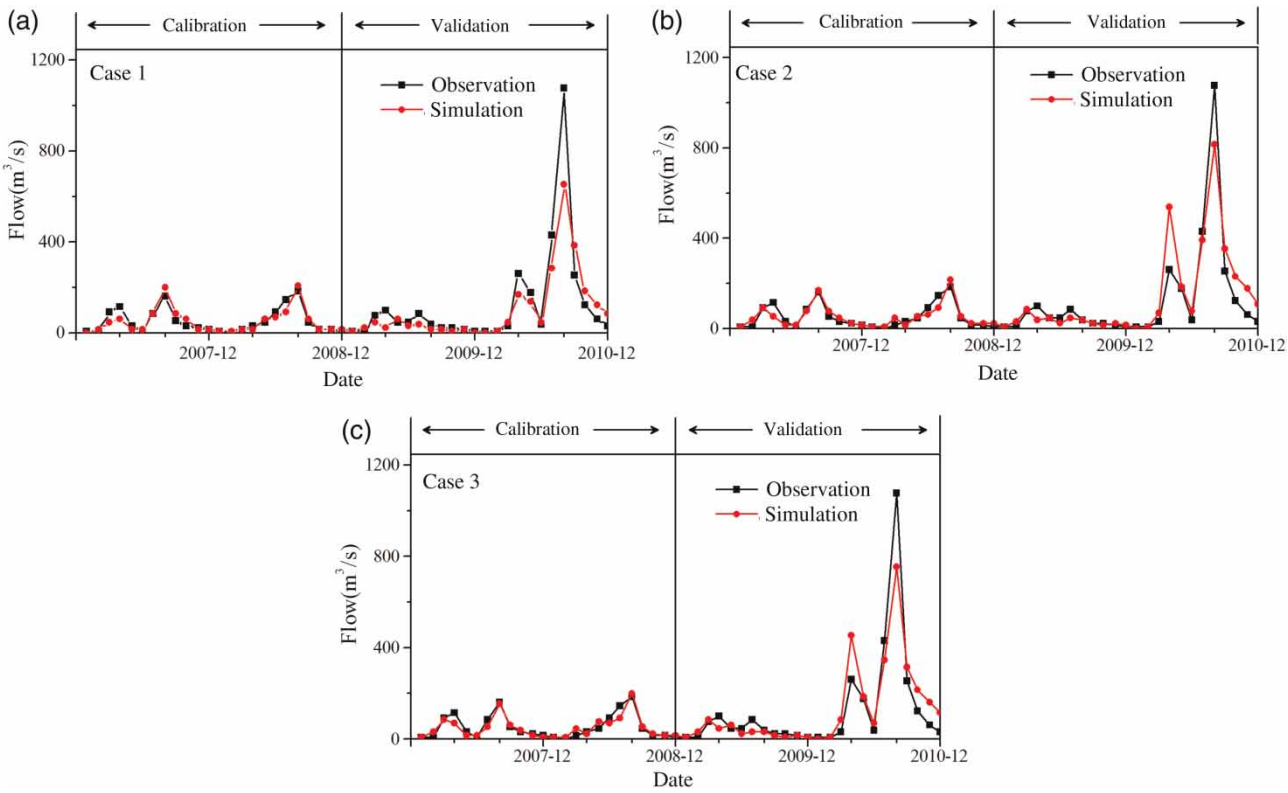

Figure 7 | Simulated streamflow by different precipitation input.

accuracy of the FY precipitation product had regional differences in China. In this paper, we have only run the model in Huifa River basin, northeast China. Our future work will discuss the performance of streamflow simulation using FY precipitation product at different time steps in different places in China.

REFERENCES

Akhavan, S., Abedi-Koupai, J., Mousavi, S.-F., Afyuni, M., Eslamian, S.-S. & Abbaspour, K. C. 2010 Application of SWAT model to investigate nitrate leaching in Hamadan–Bahar Watershed, Iran. *Agr. Ecosyst. Environ.* **139**, 675–688.

Anctil, F., Lauzon, N., Andréassian, V., Oudin, L. & Perrin, C. 2006 Improvement of rainfall-runoff forecasts through mean areal rainfall optimization. *J. Hydrol.* **328**, 717–725.

Arnold, J., Williams, J., Srinivasan, R. & King, K. 1996 *The Soil and Water Assessment Tool (SWAT) User's Manual*. Agricultural Research Service, Temple, TX.

Arnold, J. G., Srinivasan, R., Muttiah, R. S. & Williams, J. R. 1998 Large area hydrologic modeling and assessment part I: model development. *J. Am. Water Works Assoc.* **34**, 73–89.

Azimi, M., Heshmati, G. A., Farahpour, M., Faramarzi, M. & Abbaspour, K. 2013 Modeling the impact of rangeland management on forage production of sagebrush species in arid and semi-arid regions of Iran. *Ecol. Model.* **250**, 1–14.

Bitew, M. M., Gebremichael, M., Ghebremichael, L. T. & Bayissa, Y. A. 2012 Evaluation of high-resolution satellite rainfall products through streamflow simulation in a hydrological modeling of a small mountainous watershed in Ethiopia. *J. Hydrometeorol.* **13**, 338–350.

Easton, Z., Fuka, D., White, E., Collick, A., Biruk Asharge, B., McCartney, M., Awulachew, S., Ahmed, A. & Steenhuis, T. 2010 A multi basin SWAT model analysis of runoff and sedimentation in the Blue Nile, Ethiopia. *Hydrol. Earth Syst. Sci.* **7**, 3837–3878.

Jayakrishnan, R., Srinivasan, R., Santhi, C. & Arnold, J. 2005 Advances in the application of the SWAT model for water resources management. *Hydrol. Process.* **19**, 749–762.

Liu, R., Wen, J., Wang, X. & Zhang, Y. 2015 Evapotranspiration estimated by using datasets from the Chinese FengYun-2D geostationary meteorological satellite over the Yellow River source area. *Adv. Space. Res.* **55**, 60–71.

Masih, I., Maskey, S., Uhlenbrook, S. & Smakhtin, V. 2011 Assessing the impact of areal precipitation input on streamflow simulations using the SWAT Model1. *J. Am. Water. Resour. Assoc.* **47**, 179–195.

Moriasi, D., Arnold, J., Van Liew, M., Bingner, R., Harmel, R. & Veith, T. 2007 Model evaluation guidelines for systematic quantification of accuracy in watershed simulations. *Trans. ASABE* **50**, 885–900.

Nash, J. & Sutcliffe, J. 1970 River flow forecasting through conceptual models part I – a discussion of principles. *J. Hydrol.* **10**, 282–290.

Neitsch, S., Arnold, J., Kiniry, J., Williams, J. & King, K. 2005 *Soil and Water Assessment Tool: Theoretical Documentation, Version 2005*. Agricultural Research Service, Temple, TX.

Niraula, R., Kalin, L., Srivastava, P. & Anderson, C. J. 2013 Identifying critical source areas of nonpoint source pollution with SWAT and GWLF. *Ecol. Model.* **268**, 123–133.

Price, K., Purucker, S. T., Kraemer, S. R., Babendreier, J. E. & Knightes, C. D. 2014 Comparison of radar and gauge precipitation data in watershed models across varying spatial and temporal scales. *Hydrol. Process* **28**, 3505–3520.

Rasmussen, M. O., Sørensen, M. K., Wu, B., Yan, N., Qin, H. & Sandholt, I. 2014 Regional-scale estimation of evapotranspiration for the North China Plain using MODIS data and the triangle-approach. *Int. J. Appl. Earth. Obs.* **31**, 143–153.

Schaffner, M., Bader, H.-P. & Scheidegger, R. 2009 Modeling the contribution of point sources and non-point sources to Thachin River water pollution. *Sci. Total. Environ.* **407**, 4902–4915.

Schuol, J., Abbaspour, K. C., Srinivasan, R. & Yang, H. 2008 Estimation of freshwater availability in the West African sub-continent using the SWAT hydrologic model. *J. Hydrol.* **352**, 30–49.

Setegn, S., Melesse, A., Haiduk, A., Webber, D., Wang, X. & McClain, M. 2014 Modeling hydrological variability of fresh water resources in the Rio Cobre watershed, Jamaica. *Catena* **120**, 81–90.

Shen, Z., Gong, Y., Li, Y., Hong, Q., Xu, L. & Liu, R. 2009 A comparison of WEPP and SWAT for modeling soil erosion of the Zhangjiachong Watershed in the Three Gorges Reservoir Area. *Agr. Water. Manage.* **96**, 1435–1442.

Shu, Y., Stisen, S., Jensen, K. H. & Sandholt, I. 2011 Estimation of regional evapotranspiration over the North China Plain using geostationary satellite data. *Int. J. Appl. Earth. Obs.* **13**, 192–206.

Sloboda, M. & Swayne, D. 2013 Autocalibration experiments using machine learning and high performance computing. *Environ. Modell. Softw.* **40**, 302–315.

Strauch, M., Bernhofer, C., Koide, S., Volk, M., Lorz, C. & Makeschin, F. 2012 Using precipitation data ensemble for uncertainty analysis in SWAT streamflow simulation. *J. Hydrol.* **414**, 413–424.

Sun, H., Cornish, P. & Daniell, T. M. 2002 Spatial variability in hydrologic modeling using rainfall-runoff model and digital elevation model. *J. Hydrol. Eng.* **7**, 404–412.

Tobin, K. J. & Bennett, M. E. 2009 Using SWAT to model streamflow in two river basins with ground and satellite precipitation data1. *J. Am. Water. Resour. Assoc.* **45**, 253–271.

Tobin, K. J. & Bennett, M. E. 2013 Temporal analysis of Soil and Water Assessment Tool (SWAT) performance based on remotely sensed precipitation products. *Hydrol. Process.* **27**, 505–514.

Tobin, K. J. & Bennett, M. E. 2014 Impact of model complexity and precipitation data products on modeled streamflow. *J. Hydroinform.* **16**, 588–599.

Van Griensven, A., Meixner, T., Grunwald, S., Bishop, T., Diluzio, M. & Srinivasan, R. 2006 A global sensitivity analysis tool for the parameters of multi-variable catchment models. *J. Hydrol.* **324**, 10–23.

Wagner, P. D., Fiener, P., Wilken, F., Kumar, S. & Schneider, K. 2012 Comparison and evaluation of spatial interpolation schemes for daily rainfall in data scarce regions. *J. Hydrol.* **464**, 388–400.

Xu, H., Xu, C.-Y., Chen, H., Zhang, Z. & Li, L. 2013 Assessing the influence of rain gauge density and distribution on hydrological model performance in a humid region of China. *J. Hydrol.* **505**, 1–12.

Yang, J., Jiang, L., Shi, J., Wu, S., Sun, R. & Yang, H. 2014 Monitoring snow cover using Chinese meteorological satellite data over China. *Remote. Sens. Environ.* **143**, 192–203.

Yu, M., Chen, X., Li, L., Bao, A. & De la Paix, M. J. 2011 Streamflow simulation by SWAT using different precipitation sources in large arid basins with scarce raingauges. *Water. Resour. Manage.* **25**, 2669–2681.

Zhang, P., Liu, Y., Pan, Y. & Yu, Z. 2013 Land use pattern optimization based on CLUE-S and SWAT models for agricultural non-point source pollution control. *Math. Comput. Model.* **58**, 588–595.

First received 15 October 2014; accepted in revised form 5 February 2015. Available online 28 February 2015